Time-Domain Simulation of *n* Coupled Transmission Lines

FABIO ROMEO AND MAURO SANTOMAURO, MEMBER, IEEE

Abstract **—In this paper, a general SPICE model for n coupled transmission lines is presented. The model consists of two identical transformation networks and n single-transmission-line models. The transformation networks are realized with linear time-invariant voltage-controlled voltage sources (VCVS's) and current-controlled current sources (CCCS's) only. A simplified model designed to simulate connections on multilayer printed circuit boards is also presented. In this case, the coupling model is adequately described by a capacitance matrix C and an inductance matrix L that are Toeplitz, symmetric, and tridiagonal. The particular structure of C and L makes the computation of the parameters of the transformation network extremely easy and efficient because only simple function evaluations (cosines) are required. Furthermore, the transformation network depends only on the number of coupled lines and not on the parameters of those lines. Therefore, a library of such models needs to be determined only once, and only the characteristic impedances and time delays for the single lines have to be recomputed. The simulation results have been compared against experimental results, and the difference between the two is less than 1 percent.**

I. Introduction

IN THE RANGE of frequencies allowed by actual integrated devices, a connection only a few inches long has a significant influence on the quality of signal to be transmitted. In particular, connections behave like transmission lines; hence, phenomena such as reflections, impedance matching, and cross-coupling have to be considered when a connection is to be designed.

Simulators such as SPICE [1] can be used to analyze circuits (devices and connections), but while the set of models for devices is rather complete, the set of models for transmission lines is limited. In particular, only the single-line ideal model is available [2], [3] in most circuit simulators.

While the extension of the single-line model to two coupled lines is fairly simple, the generalization to more than two coupled lines is not straightforward. This topic has been addressed by several authors [2], [4]–[7] and different simulation models were presented. All of these models require the use of particular circuit models not allowed in general-purpose circuit simulators such as SPICE. Only recently in [8], a SPICE model for multiple coupled transmission lines has been presented.

The aim of this paper is to derive from the *general* model a *simplified* one that can be used in a particular but rather common setting. The parameters of this latter model are computed in a very efficient way that requires only simple transcendental function evaluations, as opposed to the computation of eigenvalues and eigenvectors that are necessary in the most general setting. Furthermore, the assumptions that have to be verified for the *simplified* model to be as accurate as the *general* one are commonly satisfied when microstrip lines on multilayer printed circuit board are considered.

The paper is organized as follows. First, a mathematical formulation of the general problem is given. Then, the simplified model is described, the limiting assumptions are introduced, and an algorithm to determine the model parameters is presented. Finally, a comparison between waveforms recorded on a real circuit and those determined by using SPICE with the *simplified* model is presented in the last section of the paper.

II. Mathematical Formulation

Let us consider a set of n coupled, lossless transmission lines. With the assumption of the *transverse electromagnetic* (TEM) mode of wave propagation, the distribution of voltages and currents along the lines is given by the generalized *telegraphists' equations* [9]

$$\begin{bmatrix} \boldsymbol{v}^x(x,t) \\ \boldsymbol{i}^x(x,t) \end{bmatrix} = -\begin{bmatrix} 0 & \boldsymbol{L} \\ \boldsymbol{C} & 0 \end{bmatrix} \begin{bmatrix} \boldsymbol{v}^t(x,t) \\ \boldsymbol{i}^t(x,t) \end{bmatrix} \tag{1}$$

where vectors $\boldsymbol{v}(x,t)$ and $\boldsymbol{i}(x,t)$ denote voltages and currents, respectively. Superscripts x and t denote differentiation of signals with respect to space and time, respectively. Distance and time are denoted by x and t. $\boldsymbol{L} = [l_{i,j}]$ is the per-unit-length (PUL) inductance matrix and

$$\boldsymbol{C} = \begin{bmatrix} c_{1,1} & -c_{1,2} & \cdots & -c_{1,n} \\ -c_{2,1} & c_{2,2} & \cdots & -c_{2,n} \\ \cdot & \cdot & \cdots & \cdot \\ \cdot & \cdot & \cdots & \cdot \\ \cdot & \cdot & \cdots & \cdot \\ -c_{n,1} & -c_{n,2} & \cdots & c_{n,n} \end{bmatrix}$$

is the PUL capacitance matrix. The matrix $\boldsymbol{C}$ is symmetric, diagonally dominant, positive definite [10] and such that

$$c_{i,i} = c_{i,0} + \sum_{\substack{j=1 \\ j \neq i}}^{n} (c_{i,j})$$

where $c_{i,0}$ is the capacitance PUL of line i with respect to ground, and $c_{i,j}$ is the capacitance PUL between line i

Manuscript received May 30, 1986, revised October 2, 1986.
F. Romeo is with the Department of Electrical Engineering and Computer Sciences, University of California, Berkeley, CA 94720, and Honeywell Information System, Italy.
M. Santomauro is with the Dipartimento di Automazione Industriale, Universitá di Brescia, Brescia, Italy.
IEEE Log Number 8611913.

0018-9480/87/0200-0131$01.00 ©1987 IEEE

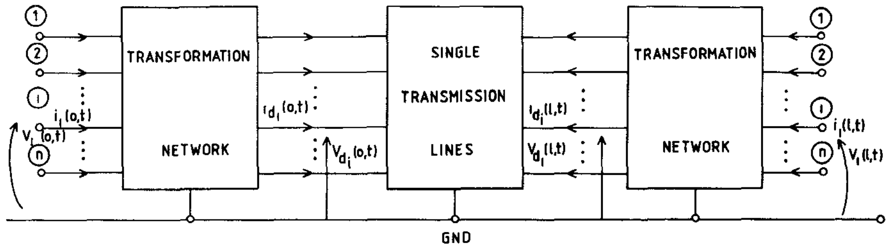

Fig. 1. Structure of the model for n coupled lines.

and line j. The matrix $\boldsymbol{L}$ is symmetric and positive definite, with $l_{i,i}$ the self-inductance PUL of line i and $l_{i,j}$ the mutual inductance PUL between line i and line j.

Given a set of coupled lines, e.g., a set of microstrips on a printed circuit board, the entries of matrices $\boldsymbol{L}$ and $\boldsymbol{C}$ can be numerically computed once the geometries of the lines and the dielectric constant of the inhomogeneous coupling material are given and the TEM mode is assumed. Algorithms to compute these parameters are well known and examples can be found in [11]–[13].

In the cases of common interest, e.g., connections on printed circuit boards, the nature of the media in which the transmission lines are embedded is such that the magnetic properties are not dependent on the type of dielectric used and are equivalent to those obtained when the dielectric is replaced by a vacuum. Bearing this in mind, the values of the entries of matrix $\boldsymbol{L}$ are computed by means of the following relation [5]:

$$\boldsymbol{L} = \boldsymbol{L}_0 = \mu_0 \epsilon_0 C_0^{-1}$$

where C_0 is the capacitance matrix for the same set of transmission lines with the dielectric replaced by a vacuum.

Let us consider now the following change of basis from $\boldsymbol{v}$ to $\boldsymbol{v}_d$ and from $\boldsymbol{i}$ to $\boldsymbol{i}_d$:

$$\boldsymbol{v} = \boldsymbol{M}_V \boldsymbol{v}_d \tag{2a}$$

$$\boldsymbol{i} = \boldsymbol{M}_I \boldsymbol{i}_d \tag{2b}$$

where $\boldsymbol{M}_I$ and $\boldsymbol{M}_V$ are n by n constant matrices. Substituting (2) into (1), we obtain

$$\begin{bmatrix} \boldsymbol{v}_d^x(x,t) \\ \boldsymbol{i}_d^x(x,t) \end{bmatrix} = -\begin{bmatrix} 0 & \boldsymbol{L}_d \\ \boldsymbol{C}_d & 0 \end{bmatrix} \begin{bmatrix} \boldsymbol{v}_d^t(x,t) \\ \boldsymbol{i}_d^t(x,t) \end{bmatrix} \tag{3}$$

where $\boldsymbol{L}_d$ and $\boldsymbol{C}_d$ are given by

$$\boldsymbol{L}_d = \boldsymbol{M}_V^{-1} \boldsymbol{L} \boldsymbol{M}_I \tag{4a}$$

$$\boldsymbol{C}_d = \boldsymbol{M}_I^{-1} \boldsymbol{C} \boldsymbol{M}_V. \tag{4b}$$

Due to the particular structure of the physical problem, a number of results can be proven.

Proposition 1: Matrices $\boldsymbol{LC}$ and $\boldsymbol{CL}$ share the same eigenvalues $\lambda_i (i = 1, 2, \cdots, n)$. The corresponding right eigenvector matrices, $\boldsymbol{M}_V$ and $\boldsymbol{M}_I$, satisfy the following equation:

$$\boldsymbol{M}_I^{-1} = \boldsymbol{M}_V^T. \tag{5}$$

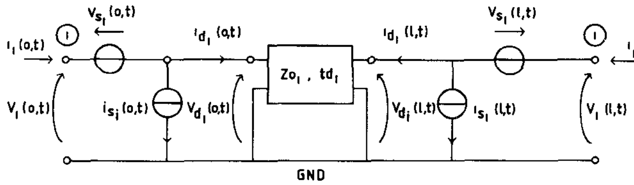

Fig. 2. Detailed model for the ith line.

Matrices $\boldsymbol{C}_d$, $\boldsymbol{L}_d$, $(\boldsymbol{LC})_d$, and $(\boldsymbol{CL})_d$ given by

$$\boldsymbol{C}_d = \boldsymbol{M}_V^T \boldsymbol{C} \boldsymbol{M}_V \tag{6a}$$

$$\boldsymbol{L}_d = \boldsymbol{M}_V^{-1} \boldsymbol{L} [\boldsymbol{M}_V^{-1}]^T \tag{6b}$$

$$(\boldsymbol{LC})_d = \boldsymbol{M}_V^{-1} \boldsymbol{L} [\boldsymbol{M}_V^{-1}]^T \boldsymbol{M}_V^T \boldsymbol{C} \boldsymbol{M}_V = \boldsymbol{L}_d \boldsymbol{C}_d \tag{6c}$$

$$(\boldsymbol{CL})_d = \boldsymbol{M}_V^T \boldsymbol{C} \boldsymbol{M}_V \boldsymbol{M}_V^{-1} \boldsymbol{L} [\boldsymbol{M}_V^{-1}]^T = \boldsymbol{C}_d \boldsymbol{L}_d \tag{6d}$$

are diagonal in the new basis obtained by (2).

Proof: A proof of (5) is given by Chang [5], while eqs. (6) follow trivially from (4) and (5). ■

The change of basis represented by (2) is the generalization of the even-mode and odd-mode decomposition to the case in which n coupled lines are considered. Equation (3) represents a set of n decoupled lines. Each of the lines propagates one and only one of the n propagation modes of the system of (1). The time-delay matrix is given by

$$\boldsymbol{W}_d = (\boldsymbol{L}_d \boldsymbol{C}_d)^{1/2} \tag{7a}$$

while the characteristic impedance matrix is given by

$$\boldsymbol{Z}_d = (\boldsymbol{L}_d \boldsymbol{C}_d)^{1/2} \boldsymbol{C}_d^{-1}. \tag{7b}$$

All the matrices in (7) are diagonal and this makes the computation of square roots and inverses trivial. Moreover, since both $\boldsymbol{W}_d$ and $\boldsymbol{Z}_d$ are diagonal matrices, the set of n coupled lines can be represented by n single lines with parameters W_{d_i} and Z_{d_i} and simulated using the single-line SPICE model. The change of basis is realized by two transformation networks, one at each end of the transmission lines model; these networks are identical because of (5).

The structure of the circuit model for n coupled lines is shown in Fig. 1, while Fig. 2 presents the detailed model for the ith line. The parameters for the circuit are obtained by the following algorithm:

Algorithm:

Step 1: Given the number of lines n, compute the eigenvalues of matrix $\boldsymbol{LC}$, λ_i.

Step 2: Compute the matrix $M_V = [M_{ij}]$ of right eigenvectors of LC.

Step 3: $i = 0$.

Step 4: $i = i+1$; compute the control law for each dependent source of the transformation network (see Fig. 2):

$$v_{s_i}(x,t) = \sum_{j=1}^{n} M_{ij} v_{d_j}(x,t) - v_{d_i}(x,t) \quad (8a)$$

$$i_{s_i}(x,t) = \sum_{i=1}^{n} M_{ij} i_{d_j}(x,t) - i_{d_i}(x,t) \quad (8b)$$

where either $x = 0$ or $x = l$, l being the length of the line.

Step 5: Compute the characteristic impedance Z_{d_i} and the time delay per unit length W_{d_i} of the ith line by (7).

Step 6: if $i < n$ go to Step 4; else stop. ∎

Equations (8) define the control laws for the VCVS and CCCS that implement the transformation network.

III. Simplified Model

To compute the transformation networks and the parameters of the system of n coupled transmission lines, the eigenvalues and the right eigenvectors of matrices LC and CL have to be computed. The complexity of the computation necessary to determine the model can be greatly reduced if a set of assumptions on the structure of the coupled lines is satisfied.

Assumption 1: The characteristics of the medium are such that both the capacitance matrix C and the inductance matrix L are n-by-n *tridiagonal* matrices, where n is the number of coupled lines. ∎

Assumption 1 introduces a constraint on the characteristics of the coupling phenomenon. In fact, the *tridiagonal* structure of the matrices implies that each transmission line is coupled directly only with the closest one to the right and with the closest one to the left. This assumption is valid in a wide variety of practical cases, in particular when the transmission lines are microstrips on a multilayer printed circuit board where every signal plane is sandwiched between two ac ground planes. Obviously, boundary effects are present and, in particular, the capacitance of the extreme transmission lines is smaller than those of the others.

Assumption 2: The lines are identical and equally spaced and side effects are negligible,[1] i.e.,

$$c_{i,i} = c, \qquad i = 1,\cdots,n$$
$$l_{i,i} = l, \qquad i = 1,\cdots,n$$
$$c_{i,j} = c_m, \qquad j = i-1, i+1, \quad i = 2,\cdots,n-1$$
$$c_{1,2} = c_{n,n-1} = c_m$$
$$l_{i,j} = l_m, \qquad j = i-1, i+1, \quad i = 2,\cdots,n-1$$
$$l_{1,2} = l_{n,n-1} = l_m.$$
∎

[1]If microstrip lines on multilayer printed circuit board are considered, the capacity of each line with respect to ground is about one order of magnitude bigger than the capacity between lines; therefore, side effects can be neglected.

These assumptions imply that both L and C are *tridiagonal* and *symmetric Toeplitz matrices*. Matrices of this form have a set of very interesting properties that allow the eigenvalues and the eigenvectors to be determined in an efficient manner that requires only cosine function evaluations.

All the required results related to Toeplitz matrices will be presented as propositions. Proofs will be omitted whenever a direct reference is available.

Proposition 2: Let T be a matrix of order n defined as follows:

$$t_{i,j} = 1, \qquad j = i-1, i+1, \quad i = 2,\cdots,n-1 \quad (9a)$$
$$t_{1,2} = t_{n,n-1} = 1 \quad (9b)$$
$$t_{i,j} = 0, \qquad \text{otherwise.} \quad (9c)$$

The characteristic polynomial of T, $\phi_n(\mu)$, is given by the following recursive equation:

$$\phi_k(\mu) = \mu\phi_{k-1}(\mu) - \phi_{k-2}(\mu), \qquad k = 2,\cdots,n \quad (10)$$

with the initial conditions

$$\phi_0(\mu) = 1 \quad (11a)$$
$$\phi_1(\mu) = \mu. \quad (11b)$$

Proof: A proof of the proposition is given in [14].

The particular structure of T, given by (9) allows for the computation of its eigenvalues without solving the characteristic equation

$$\det(\lambda I - T) = \phi_n(\mu) = 0$$

as stated in the following proposition.

Proposition 3: The solutions to the equation

$$\phi_n(\mu) = 0$$

where $\phi_n(\mu)$ is given by (10) and (11), are given by

$$\mu_i = -2\cos\frac{i\pi}{n+1}, \qquad i = 1,\cdots,n. \quad (12)$$

Proof: A proof of the proposition is given in [15]. ∎

Matrix T plays a crucial role in determining the eigenvalues of Toeplitz matrices that are also symmetric and tridiagonal.

Proposition 4: Let A be a symmetric, tridiagonal Toeplitz matrix. The eigenvalues of A are given by

$$\lambda_i(A) = a + \mu_i(T) b \quad (13)$$

where a is the element on the main diagonal of A, b is the element on the secondary diagonal of A, and $\mu_i(T)$ are the eigenvalues of matrix T.

Proof: The proof consists of showing that the eigenvalues of A can be expressed as in (13). Let us consider the following expression for A:

$$A = Ia + Tb.$$

Writing the characteristic equation for A, we obtain

$$\det(\lambda I - A) = \det((\lambda - a)I - bT) = 0. \quad (14)$$

Since by assumption

$$b \neq 0$$

by the properties of determinants, (14) can be rewritten as

$$b \det\left(\frac{(\lambda - a)}{b} \boldsymbol{I} - \boldsymbol{T}\right) = 0$$

from which (13) follows immediately. ■

Proposition 4 states that eigenvalues of every symmetric, tridiagonal Toeplitz matrix can be computed starting from the eigenvalues of matrix $\boldsymbol{T}$ by evaluation of (13). Furthermore, solutions of the characteristic equation have to be computed only once for all matrices of a given order.

The particular features of tridiagonal, symmetric Toeplitz forms are again helpful in the computation of eigenvectors necessary to diagonalize a matrix.

Proposition 5: The matrix $\boldsymbol{M}$ of right eigenvectors of $\boldsymbol{T}$ is given by

$$M_{ij} = \frac{\phi_{i-1}(\mu_j(\boldsymbol{T}))}{\gamma_j}, \qquad i, j = 1, \cdots, n \tag{15a}$$

where the normalizing factors

$$\gamma_j^2 = \sum_{i=1}^{n} \left(\phi_{i-1}(\mu_j(\boldsymbol{T}))\right)^2 \tag{15b}$$

are introduced to obtain

$$\sum_{i=1}^{n} M_{ij}^2 = 1. \tag{15c}$$

Proof: A proof of the proposition is given in [14].

Proposition 6: Matrices $\boldsymbol{A}$ and $\boldsymbol{T}$ have the same eigenvectors.

Proof: Let $\boldsymbol{x}$ be a right eigenvector of $\boldsymbol{A}$. From the definition of eigenvector and from Proposition 4 follows

$$(\lambda \boldsymbol{I} - \boldsymbol{A})\boldsymbol{x} = b\left(\frac{(\lambda - a)}{b}\boldsymbol{I} - \boldsymbol{T}\right)\boldsymbol{x} = 0.$$

Therefore

$$(\mu \boldsymbol{I} - \boldsymbol{T})\boldsymbol{x} = 0$$

which completes the proof. ■

Propositions 5 and 6 are crucial because they state two extremely important facts. The first one is that, given a matrix that is symmetric, tridiagonal, and Toeplitz, the eigenvector matrix $\boldsymbol{M}$ can be determined without solving any system of equations. The second is that the transformation matrix is related only to the order of the matrix to be transformed and not to values of its nonzero elements. From this latter remark follows the useful result below.

Proposition 7: Since $\boldsymbol{L}$ and $\boldsymbol{C}$ are symmetric, tridiagonal, Toeplitz matrices, the same transformation matrix $\boldsymbol{M}$ diagonalizes both $\boldsymbol{L}$ and $\boldsymbol{C}$; as a consequence, it follows that

$$\boldsymbol{M}^{-1}\boldsymbol{L}\boldsymbol{M}\boldsymbol{M}^{-1}\boldsymbol{C}\boldsymbol{M} = \boldsymbol{M}^{-1}\boldsymbol{L}\boldsymbol{C}\boldsymbol{M}$$

and then $\boldsymbol{M}$ diagonalizes $\boldsymbol{LC}$ also.

Proof: The proof follows immediately from Proposition 6. ■

The algorithm described in Section II is now simplified as follows:

Simplified Algorithm:

Step 1: Given the number of lines n, compute the eigenvalues of $\boldsymbol{T}$ by (12).

Step 2: Compute the matrix $\boldsymbol{M}$ of right eigenvectors of $\boldsymbol{T}$ by (15).

Step 3: $i = 0$.

Step 4: $i = i + 1$; compute the control law for each dependent source (see fig. 2)

$$v_{s_i}(x,t) = \sum_{j=1}^{n} M_{ij} v_{d_j}(x,t) - v_{d_i}(x,t) \tag{16a}$$

$$i_{s_i}(x,t) = \sum_{j=1}^{n} M_{ij} i_{d_j}(x,t) - i_{d_i}(x,t) \tag{16b}$$

where either $x = 0$ or $x = l$, l being the length of the line.

Step 5: Compute the characteristic impedance Z_{d_i} and the time delay W_{d_i} of line i

$$Z_{d_i} = \left(\frac{l + \mu_i(\boldsymbol{T}) l_m}{c - \mu_i(\boldsymbol{T}) c_m}\right)^{1/2} \tag{17a}$$

$$W_{d_i} = \left[(l + \mu_i(\boldsymbol{T}) l_m)(c - \mu_i(\boldsymbol{T}) c_m)\right]^{1/2}. \tag{17b}$$

Step 6: if $i < n$ go to Step 4; else stop.

Remark 1: The computation of Step 1 and of Step 2 depends only on the number of lines and so is executed only once; as a consequence, the model for different sets of n lines requires the computation of Step 5 only.

Remark 2: If $n = 2$, the model presented here reduces to the usual model for two coupled lines. In particular, the odd mode is propagated by the first line while the even mode is propagated by the second one. It is important to note that in this case Assumption 1 and Assumption 2 have no effect since both lines are boundary lines and hence no approximation is used. ■

Parameters l, l_m, c, and c_m have to be determined either by measurements[2] or by computations starting from the geometrical dimension of the lines. For the sake of simplicity, the second approach has been followed.

A computer program to evaluate electrical parameters and to determine the model of coupled lines based on the above Simplified Algorithm has been designed. The program computes l, l_m, c, and c_m starting from the geometrical dimensions of the microstrip lines using the algorithms presented in [11], and [12]. Then, the transmission-line parameters W_{d_i}, Z_{d_i}, and the transformation networks are computed with (16) and (17). The output is generated using the SPICE input syntax and it is stored in a file as a SPICE subcircuit model.

[2] The procedure is rather delicate since the measurements are error-prone.

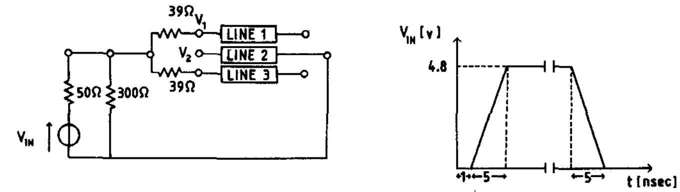

Fig. 3. Circuit example.

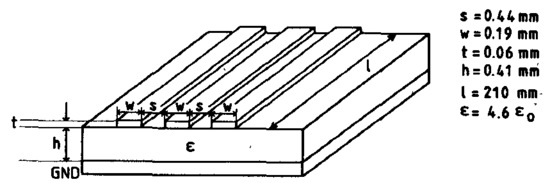

Fig. 4. Geometry of three coupled lines.

IV. Example of Application

The model presented in the previous section has been applied to study three coupled lines on a multilayer printed circuit board. The circuit, shown in Fig. 3, represents a simplified version of a data bus. In Fig. 4 the geometrical characteristics of microstrips are listed.

The simplified model was simulated with SPICE and the results were compared with two photographs taken with a 500-MHz oscilloscope. Figs. 5 and 6 show simulated and measured node voltages $v_1(t)$ and $v_2(t)$ when a rising step (a) and a falling step (b) are applied by the voltage source V_{in}.

The agreement between the measured and simulated voltages is very good; the maximum difference between the two voltages is less than 1 percent. The time required to simulate the circuit was about 20 min of CPU time on a Honeywell L 66/80 computer for each transient, while the time required to determine the model parameters was less than 1 s.

A comment is in order with respect to HSPICE [16], the particular version of SPICE used to perform the simulation. When a transmission line is simulated in the time domain, if the line is not perfectly matched at both ends, reflection waves are generated every W_d time units. Since the transmission line is lossless, no distortion or attenuation is introduced; this means that if the input signal presents a break point[3] another one will be created every time a reflection occurs. As a consequence, the resulting time step can be extremely small. This effect is even more evident when coupled lines are simulated. In this case, every line has its own W_d; hence, in general, break points occur at different times for each line. To handle these problems, HSPICE has a modified algorithm to control the generation of break points and the computation of the time step in the vicinity of break points [17]. In particular, when transmission lines are simulated, only a limited number of reflections are considered for the generation of break points. Furthermore, the minimum time step around the break point is controlled adaptively by the user so that a good tradeoff between accuracy and speed is achieved. Several runs were performed to test the accuracy of the simulation with different time step control strategies and no significant differences in the waveform were detected. In contrast, several CPU hours were required to complete the simulation of the same test case with the standard control strategy.

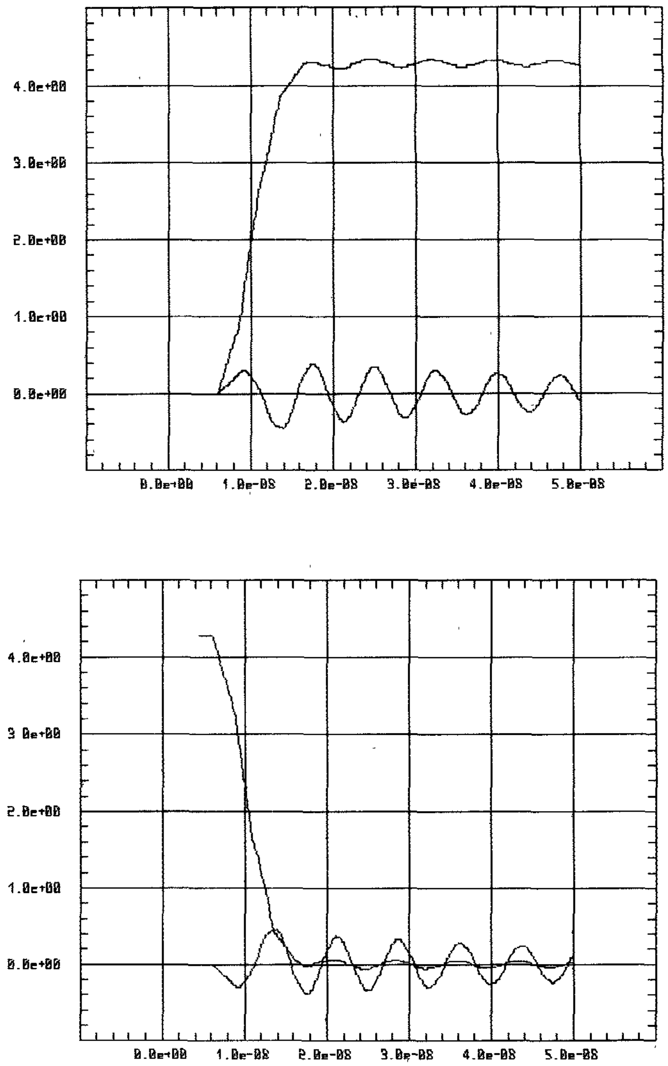

Fig. 5. Node voltages obtained by SPICE.

Finally, the measured values of capacitances c_{ii} and c_{ij} with $i \neq j, i, j = 1,2,3$, are presented below together with the corresponding computed values (listed in parentheses)

$$c_{11} = c_{10} + c_{12} = 68.8 \text{ pF/m} \qquad (68.6 \text{ pF/m})$$
$$c_{22} = c_{20} + c_{21} + c_{23} = 75.5 \text{ pF/m} \qquad (76.6 \text{ pF/m})$$
$$c_{33} = c_{30} + c_{32} = 68.8 \text{ pF/m} \qquad (68.6 \text{ pF/m})$$
$$c_{12} = c_{21} = c_{23} = c_{32} = 6.7 \text{ pF/m} \qquad (8.0 \text{ pF/m}).$$

The measured values of the capacitances were obtained by

[3]A break point is a time point in which a waveform undergoes a sharp change in its first time derivative. In coincidence with such points, SPICE reduces its time step so that the next time step will be coincident with the break point [1].

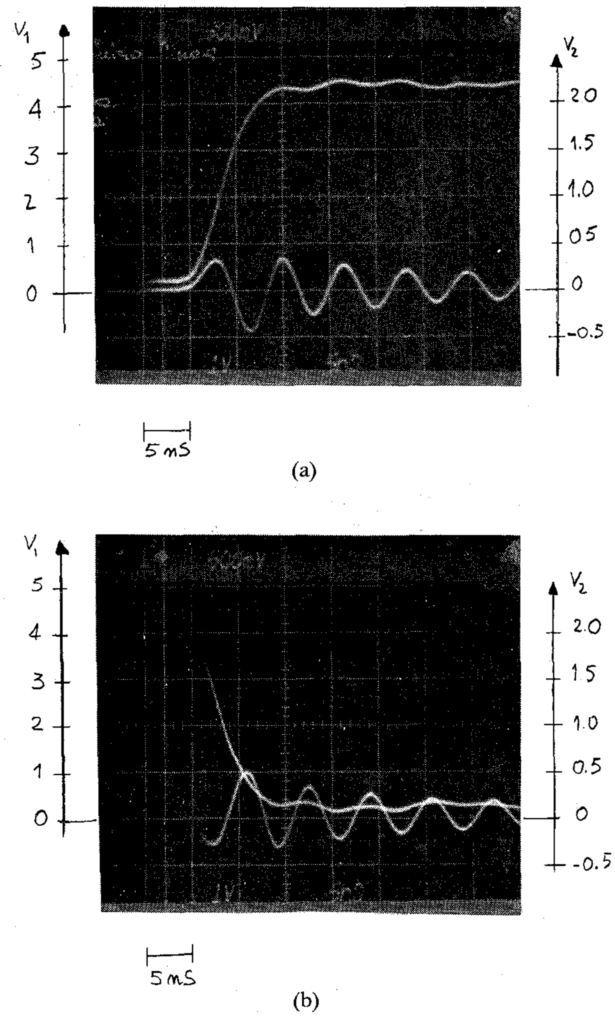

Fig. 6. Node voltages obtained by measurements.

solving the following system of equations:

$$c_{10} + c_{12} = c_{M_1}$$
$$c_{12} + c_{20} + c_{23} = c_{M_2}$$
$$c_{23} - c_{12} = 0$$

where c_{M_1} is the capacitance measured at one end of line 1 when line 2 is grounded, and c_{M_2} is the capacitance measured at one end of line 2 when both line 1 and line 3 are grounded. The computed values of capacitances were determined by means of the program described at the end of the previous section. The results show an order of magnitude of difference between c_{i0} and $c_{ij}, i \neq j$, which proves that Assumption 2 is fulfilled to a good approximation.

A number of tests are presently in progress to check the agreement between the results predicted by the program and measurements for an extended range of microstrip dimensions.

V. Conclusions

A simplified simulation model for a set of coupled lines has been presented. The construction of the model is based on two assumptions on the characteristics of the coupling phenomenon. The assumptions are usually satisfied for microstrip lines constructed on multilayer printed circuit boards.

To determine the model parameters, only function evaluations are required. The transformation networks necessary at both ends of the model are dependent on the number of coupled lines only and can be determined once. Only two parameters for each line have to be computed to simulate sets of coupled lines with different parameters.

The test case presented shows good agreement between the results obtained with the simulation and those obtained by testing a real circuit with a high-resolution oscilloscope. The errors in voltages were less than 1 percent.

Acknowledgment

Many suggestions have been useful to complete this study. In particular, the authors wish to acknowledge Prof. C. Desoer and Prof. V. Amoia for many helpful discussions on the subject of the paper. The help of C. Parolo and M. Torno of Honeywell Information System Italia was determinant to complete measurements in the real case.

References

[1] L. W. Nagel, "SPICE2: A computer program to simulate semiconductor circuits," Memo. No. M520 Elect. Res. Lab., Elect. Res. Lab., College of Engineering, Univ. of California, Berkeley, CA 94720, 1975.

[2] F. H. Branin, "Transient analysis of lossless transmission lines," *Proc. IEEE*, vol. 55, pp. 2012–2013, 1967.

[3] A. E. Ruehli, "Survey of computer-aided electrical analysis of integrated circuit interconnections," *IBM J. Res. Devel.*, vol. 23, no. 6, pp. 626–639 , 1979.

[4] H. Amemiya, "Time domain analysis of multiple parallel transmission lines," *RCA Rev.*, vol. 28, pp. 241–276, 1967.

[5] F. Chang, "Transient analysis of lossless coupled transmission lines in a nonhomogeneous dielectric medium," *IEEE Trans. Microwave Theory Tech.*, vol. MTT-18, no. 9, pp. 616–626, 1970.

[6] R. Daumas, D. Pompei, E. Rivier, and A. Ross, "Extension de la Theorie de Kirchhoff aux Lignes Rubans Couplees Application au Calcul des Coupleurs en Lignes a Bandes," *Annales des Telecommunications*, vol. 28, no. 7–8, pp. 325–334, 1973.

[7] C. W. Ho, "Theory and computer-aided analysis of lossless transmission lines," *IBM J. Res. Develop.*, vol. 17, pp. 249–255, 1973.

[8] V. K. Tripathi and J. B. Rettig, "A SPICE model for multiple-coupled microstrips and other transmission lines," *1985 IEEE MTT-S Dig.*, pp. 703–706, 1985.

[9] P. C. Magnusson, *Transmission Lines and Wave Propagation.* Newton, MA: Allyn and Bacon, 1970.

[10] R. M. Fano, L. J. Chu, and R. B. Adler, *Electromagnetic Fields, Energy, and Forces.* New York: John Wiley & Sons, 1960.

[11] K. C. Gupta, R. Garg, and I. J. Bahl, *Microstrip Lines and Slotlines.* Dedham, MA: Artech House, 1979.

[12] M. V. Schneider, "Microstrip lines for microwave integrated circuits," *The Bell Syst. Tech. J.*, pp. 1421–1444, 1969.

[13] T. C. Edwards, *Foundation for Microstrip Circuit Design.* New York: John Wiley & Sons, 1983.

[14] J. N. Franklin, *Matrix Theory.* Englewood Cliffs, NJ: Prentice Hall, 1968.

[15] U. Grenader and G. Szego, *Toeplitz Forms and Their Application.* University of California Press, Berkeley and Los Angeles, 1958.

[16] J. C. Lai, *HSPICE User's Manual, Honeywell Circuit Simulation Program*, Honeywell Solid-State Electronics Division, Minneapolis, MN, 1981.

[17] D. Bauer, "A review of the wiring rules and circuit simulators used for printed circuit board design," in *Proc. 4th Ann. Honeywell CAD&CAM Workshop*, Minneapolis, MN, Oct. 1982.

Mauro Santomauro (M'74) was born in Imperia, Italy, in February 1947. He received the Dr. Eng. degree from the Politecnico di Milano, Italy, in 1971.

From 1971 to 1986, he was with the Dipartimento di Elettronica del Politecnico di Milano, where he held the positions of Research Associate, Assistant Professor, and Associate Professor. In 1986, he joined the Dipartimento di Automazione Industriale at the University of Brescia, where he is presently Professor of Electrical Network Theory. In 1982 (August–December) and in 1983 (July–November), he was a Research Associate at the Department of Electrical Engineering and Computer Sciences at the University of California at Berkeley. His research interests are in computer-aided-design of electronic circuits and systems, with particular emphasis on layout problems, circuit simulation, and logic minimization.

Dr. Santomauro is a member of the Associazione Elettrotecnica ed Elettronica Italiana (AEI).

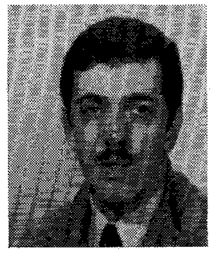

Fabio Romeo received the Dr. Eng. degree from the Politecnico di Milano, Italy, in 1979.

From 1980 to 1982, he was with the Instituto di Elettrotecnica ed Elettronica, Politecnico di Milano, where he held the position of Research Associate. In 1982, he joined the Research and Development Department of Honeywell Information System Italy. Presently, he is with the Department of Electrical Engineering and Computer Sciences at the University of California, Berkeley, where he is working toward the Ph.D. degree. His research interests include several aspects of the computer-aided design of integrated circuits, with particular emphasis on automatic layout of integrated circuits and probabilistic optimization algorithms.

Dr. Romeo was awarded with the Italian Research Council Fellowship in 1983, and the Honeywell Technical Award in 1984.